AD-A060 378 MARYLAND UNIV COLLEGE PARK DEPT OF PHYSICS AND ASTRONOMY F/G 18/1
STABILITY PROPERTIES OF A CYLINDRICAL ROTATING P-LAYER IMMERSED--ETC(U)
1978 H S UHM, R C DAVIDSON N00014-75-C-0309

UNCLASSIFIED NL

1 OF 1
AD
A060378

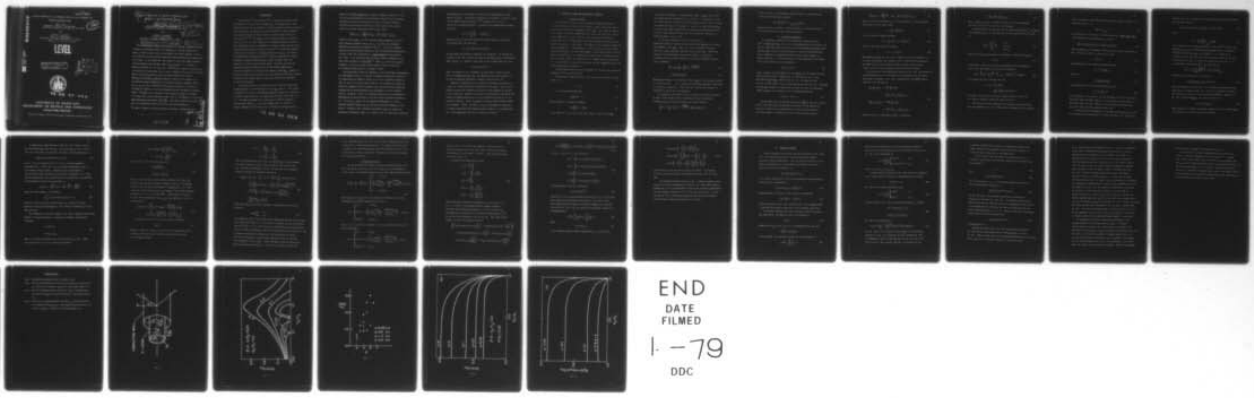

END
DATE
FILMED
1-79
DDC

PREPRINT #806P002

STABILITY PROPERTIES OF A CYLINDRICAL ROTATING P-LAYER IMMERSED IN A UNIFORM BACKGROUND PLASMA

Han S. Uhm
Department of Physics and Astronomy
University of Maryland, College Park, Md. 20742

and

Ronald C. Davidson*
Office of Fusion Energy
Department of Energy, Washington, D. C. 20545

N00014-75-C-0309

LEVEL II

UNIVERSITY OF MARYLAND
DEPARTMENT OF PHYSICS AND ASTRONOMY
COLLEGE PARK, MARYLAND

*On leave of absence from the University of Maryland, College Park, Md.

STABILITY PROPERTIES OF A CYLINDRICAL ROTATING P-LAYER IMMERSED IN A UNIFORM BACKGROUND PLASMA

Han S. Uhm
Department of Physics and Astronomy
University of Maryland, College Park, Md. 20742

and

Ronald C. Davidson*
Office of Fusion Energy
Department of Energy, Washington, D. C. 20545

N0001 4-75-C-0309

The electrostatic stability properties of a rotating, charge-neutralized P-layer are investigated within the framework of a hybrid (Vlasov-fluid) model in which the layer ions are described by the Vlasov equation, and the layer electrons and the uniform background plasma are described as macroscopic, cold fluids. It is assumed that the P-layer is thin, with radial thickness (2a) much smaller than the mean radius (R_0), and that $\nu \ll 1$, where ν is Budker's parameter for the layer ions. Electrostatic stability properties are calculated for perturbations about a weakly diamagnetic P-layer with rectangular density profile, described by the equilibrium distribution function $f_b^0=(n_b R_0/2\pi m_i)\delta[H-V_z P_z-m_i(V_0^2-V_z^2)/2]\delta(P_\theta-P_0)$, where H is the energy, P_θ is the canonical angular momentum, P_z is the axial canonical momentum, and n_b, R_0, V_z, V_0, and P_0 are constants. The stability analysis is carried out including the effects of a uniform background plasma, and weak self magnetic fields. Although a slow rotational P-layer ($P_0>0$) is found to be stable, it is shown that a fast rotational P-layer ($P_0 < 0$) is unstable for sufficiently high background plasma density ($\omega_p^2 \gg \omega_{ci}^2$). The typical instability growth rate is a substantial fraction of the ion cyclotron frequency.

*On leave of absence from the University of Maryland, College Park, Md.

I. INTRODUCTION

The generation[1-6] and application[7-9] of intense ion beams has been the subject of several recent investigations. One application of considerable interest is the formation of field-reversed ion layers and rings,[7-9] which can provide the magnetic confinement geometry for fusion plasmas. Such layers and rings are likely subject to various macro- and micro-instabilities.[10-16] For example, the low frequency stability properties ($|\omega| << \omega_{ci}$) of an ion layer immersed in a background plasma have recently been investigated within the framework of a kinetic energy principle that incorporates the effects of large ion orbits.[11] In the present analysis, allowing for perturbations of moderate frequency ($|\omega| \sim \omega_{ci}$), we examine the equilibrium and negative-mass[12-15] stability properties of a weakly diamagnetic, charge-neutralized proton layer (P-layer) within the framework of a hybrid (Vlasov-fluid) model. The layer electrons and background plasma electrons and ions are described as macroscopic, cold fluids immersed in a uniform axial magnetic field $B_0\hat{e}_z$. However, to correctly include the influence of layer ion dynamics on stability behavior, we adopt a fully kinetic model in which the layer ions are described by the Vlasov equation.

The present analysis is carried out for an infinitely long P-layer aligned parallel to a uniform magnetic field $B_0\hat{e}_z$ (Fig. 1). The P-layer is immersed in a uniform, cylindrical background plasma and is charge neutralized by extra electrons. We assume that the layer is thin [Eq. (1)], i.e., the radial thickness (2a) of the layer is small in comparison with the mean radius R_0. It is also assumed that $\nu << 1$, where ν is Budker's parameter for the layer ions. Although the equilibrium self

magnetic field $B^s_{0\theta}(r)\hat{e}_\theta + B^s_{0z}(r)\hat{e}_z$ is weak in absolute intensity for $\nu \ll 1$, the self-field gradients can be sufficiently large to have an important influence on particle trajectories, and hence on stability behavior. Equilibrium and stability properties are calculated for the specific choice of ion layer distribution function [Eq. (10)],

$$f_b^0(H,P_z,P_\theta) = \frac{n_b R_0}{2\pi m_i}\,\delta\left(H - V_z P_z - \frac{m_i}{2}\,(V_0^2 - V_z^2)\right)\,\delta(P_\theta - P_0)\ ,$$

where H is the energy, P_θ is the canonical angular momentum, P_z is the axial canonical momentum, and n_b, R_0, V_z, V_0, and P_0 are constants. Equilibrium properties are examined in Sec. II. One of the important features of the equilibrium analysis is that the equilibrium distribution function in Eq. (10) corresponds to a sharp-boundary density profile [Eq. (29)]. It is also found that the radial betatron frequency of the layer ions is given by $\omega_r = (\omega_{ci}^2 + \omega_b^2\beta^2)^{1/2}$, where ω_{ci} is the ion cyclotron frequency, ω_b is the ion layer plasma frequency, and β is the ratio of the mean ion layer speed to the speed of light.

The electrostatic stability properties of the layer-plasma configuration are investigated in Secs. III and IV, including the important influence of: (a) equilibrium self magnetic fields, (b) an outer cylindrical conductor (Fig. 1), and (c) ion layer kinetic effects. The analysis is carried out within the framework of the linearized Vlasov-fluid and Poisson equations, assuming that perturbed quantities are independent of axial coordinate ($\partial/\partial z = 0$). Moreover, in Sec. IV, stability properties are investigated for eigenfrequencies near multiples of the mean P-layer rotational frequency, i.e., $|\omega - \ell\omega_\theta| \ll \omega_{ci}$, where ω is the complex eigenfrequency, ℓ is the azimuthal harmonic number and ω_θ is the mean rotational frequency of the P-layer. Although a slow rotational equilibrium ($P_0 > 0$) is stable [see discussion following Eq. (55)], it is shown in Sec. IV that a fast rotational

equilibrium ($P_0<0$) is unstable for sufficiently high background plasma density ($\omega_p^2>>\omega_{ci}^2$). The physical mechanism for instability is similar to that for the negative-mass instability,[12-15] including the dielectric effects of the background plasma. Introducing the dimensionless parameters [Eq. (60)]

$$y=(\ell^2-1)\,\frac{n_b}{n_p}\,\frac{\omega_{ci}^2}{\omega_r^2}\,, \qquad q=\omega_b^2\beta^2/\omega_{ci}^2,$$

where n_b and n_p are the layer density and plasma density, respectively, we find that [Eqs. (62) and (63)]

$$y\leq 1, \text{ and } (1+q)y^2-(3q/2+1)y+q>0\,,$$

are necessary and sufficient conditions for instability. The instability condition in Eq. (62) is valid only when the parameter n_b/n_p is sufficiently small ($n_b/n_p<<1$). Moreover, the system is most unstable when [Eq. (65)]

$$(n_b/n_p)=(1+q)/(\ell^2-1)\,,$$

which corresponds to $y=1$. Evidently, the mean motion of the ion layer (β^2), the background plasma (n_p), and equilibrium self field effects (q), all have an important influence on stability behavior (Sec. IV).

Numerical investigations of the stability properties are carried out in Sec. IV. Several points are noteworthy in this regard. First, the instability growth rate increases when the self-field strength (as measured by q) is increased. Moreover, the system is stabilized as q approaches zero. Second, the maximum growth rate can be a substantial fraction of the ion cyclotron frequency. Third, the number of unstable modes increase rapidly as q increases. Fourth, the range of n_b/n_p corresponding to instability is rapidly reduced when the azimuthal harmonic number ℓ is increased above $\ell=2$. [The fundamental mode ($\ell=1$) is found to be stable.]

II. THEORETICAL MODEL AND EQUILIBRIUM PROPERTIES

A. Theoretical Model

As illustrated in Fig. 1, the equilibrium configuration consists of a nonrelativistic P-layer that is infinite in axial extent and aligned parallel to a uniform applied magnetic field $B_0\hat{e}_z$. The P-layer is immersed in a uniform, cylindrical background plasma (with outer radius R_c), and is charge neutralized by extra electrons with density profile identical to the layer ions. The mean radius and radial thickness of the P-layer are denoted by R_0 and $2a$, respectively. The radius of the cylindrical conducting wall is denoted by R_c. The mean motion of the P-layer is in the azimuthal and axial directions, and the applied magnetic field provides radial confinement of the layer ions. For simplicity, we assume that the plasma and layer ions are singly charged. As shown in Fig. 1, cylindrical polar coordinates (r,θ,z) are introduced, and the following are the main assumptions pertaining to the equilibrium configuration:

(a) Equilibrium properties are independent of z ($\partial/\partial z=0$) and azimuthally symmetric ($\partial/\partial\theta=0$) about the z-axis.

(b) The radial thickness of the P-layer is much smaller than its major radius, i.e.,

$$a \ll R_0 \ . \tag{1}$$

(c) It is further assumed that

$$\nu = N_b e^2/m_i c^2 \ll 1 \tag{2}$$

where $\nu = N_b e^2/m_i c^2$ is Budker's parameter,

$$N_b = 2\pi \int_0^{R_c} dr\ r\ n_b^0(r) \tag{3}$$

is the number of layer ions per unit axial length of the P-layer, $n_b^0(r)$

is the layer ion density, c is the speed of light in vacuo, and e and m_i are charge and mass, respectively, of a layer ion. The inequality in Eq. (2) implies that the intensity of the self magnetic field is much less than the applied field B_0 (i.e., $\Delta B_0/B_0 << 1$). However, the self-field gradients over the narrow radial dimension of the layer can be sufficiently strong to have a large influence on the layer ion trajectories, and hence on stability behavior (Sec. III.A).

In the present analysis, the layer electrons and background plasma are treated as cold ($T_j \to 0$) fluids immersed in a uniform axial magnetic field $B_0 \hat{e}_z$. Here, j=e', e, and i represent the layer electrons, plasma electrons, and plasma ions, respectively. Within the context of the electrostatic approximation ($\nabla \times E \simeq 0$), the equation of motion and the continuity equation for each fluid component (j=e', e, i) can be expressed as

$$\left(\frac{\partial}{\partial t} + V_j \cdot \nabla\right) V_j = \frac{e_j}{m_j}\left(-\nabla\phi + \frac{V_j \times B_0(x)}{c}\right), \tag{4}$$

$$\frac{\partial}{\partial t} n_j + \nabla \cdot (n_j V_j) = 0 , \tag{5}$$

where $E(x,t) = -\nabla\phi(x,t)$ is the electric field, $n_j(x,t)$ is the density, $V_j(x,t)$ is the mean velocity, and e_j and m_j are the charge and mass, respectively, of a particle of species j. In Eq. (4), the electrostatic analysis is consistent to the low beta approximation.

To include the influence of layer ion dynamics on stability behavior, we adopt a fully kinetic model in which the ion layer distribution function $f_b(x,v,t)$ evolves according to the Vlasov equation

$$\left(\frac{\partial}{\partial t} + v \cdot \frac{\partial}{\partial x} + \frac{e}{m_i}\left(-\nabla\phi + \frac{v \times B_0(x)}{c}\right) \cdot \frac{\partial}{\partial v}\right) f_b(x,v,t) = 0 . \tag{6}$$

In Eqs. (4)-(6), the electrostatic potential $\phi(\underset{\sim}{x},t)$ is determined self-consistently from Poisson's equation

$$\underset{\sim}{\nabla}^2\phi=-4\pi\left[e\int d^3p\ f_b + \sum_{j=e',e,i} e_j n_j(\underset{\sim}{x},t)\right] . \tag{7}$$

Equations (4)-(7) constitute a closed description of the system and form the theoretical basis for the subsequent analysis.

B. Equilibrium Properties

For azimuthally symmetric equilibrium profiles characterized by $n_j^0(r)$ and $\underset{\sim}{V}_j^0(\underset{\sim}{x})=V_{j\theta}^0(r)\hat{\underset{\sim}{e}}_\theta$, $j=e',e,i$, it is straightforward to show from Eq. (5) that the functional form of the electron layer and background plasma density profiles $n_j^0(r)$ can be specified arbitrarily. Moreover, from equilibrium charge neutrality, the equilibrium radial electric field vanishes, i.e., $E_r^0(r)=-\partial\phi^0(r)/\partial r=0$. It follows from Eq. (4) that equilibrium force balance in the radial direction can be expressed as

$$\omega_j(\omega_j+\varepsilon_j\omega_{cj})=0 , \tag{8}$$

where $\varepsilon_j=\mathrm{sgn}e_j$, and $\omega_j(r)=V_{j\theta}^0(r)/r$ and $\omega_{cj}=eB_0/m_jc$ are the angular velocity and cyclotron frequency, respectively. In obtaining Eq. (8), we have approximated $\underset{\sim}{B}_0(\underset{\sim}{x})=B_0\hat{\underset{\sim}{e}}_z$ consistent with Eq. (2). In general we note from Eq. (8) that there are two allowed equilibrium values of $\omega_j(r)$. Throughout the subsequent analysis we assume that the layer electrons and background plasma components are rotating in the slow rotational mode with

$$\omega_j(r)=0 , \quad j=e',e,i . \tag{9}$$

For the layer ions, any distribution function $f_b^0(\underset{\sim}{x},\underset{\sim}{v})$ that is a function only of the single-particle constants of the motion in the equilibrium fields is a solution to the steady-state ($\partial/\partial t=0$) ion Vlasov equation. For present purpose, we assume an ion layer equilibrium described by

$$f_b^0(H,P_z,P_\theta) = \frac{n_b R_0}{2\pi m_i}\,\delta\left(H - V_z P_z - \frac{m_i}{2}\,(V_0^2 - V_z^2)\right)\delta(P_\theta - P_0), \tag{10}$$

where V_z and V_0 are constants, n_b is the layer density at the equilibrium radius $r=R_0$, H is the total energy,

$$H = \frac{1}{2m_i}\,(p_r^2 + p_\theta^2 + p_z^2)\ , \tag{11}$$

P_θ is the canonical angular momentum,

$$P_\theta = r\left(p_\theta + \frac{m_i}{2}\,\omega_{ci} r + \frac{e}{c}\,A_\theta^s(r)\right)\ , \tag{12}$$

and P_z is the axial canonical momentum,

$$P_z = p_z + \frac{e}{c}\,A_z^s(r)\ . \tag{13}$$

Here, $A_\theta^s(r)$ and $A_z^s(r)$ are the θ- and z-components of vector potential for the axial and azimuthal self magnetic fields. Without loss of generality, we assume that the vector potentials $A_\theta^s(r)$ and $A_z^s(r)$ vanish at $r=R_0$. In Eqs. (11)-(13), lower case $\underset{\sim}{p}=m_i\underset{\sim}{v}$ denotes mechanical momentum.

For the choice of ion distribution function in Eq. (10), the equilibrium vector potentials are to be calculated self-consistently from the steady-state Maxwell equations. The θ- and z-components of the $\underset{\sim}{\nabla}\times\underset{\sim}{B}_0^s(\underset{\sim}{x})$ Maxwell equation can be expressed as

$$\begin{aligned}
\frac{\partial}{\partial r}\,\frac{1}{r}\,\frac{\partial}{\partial r}\,rA_\theta^s(r) &= -\frac{4\pi e}{c}\,n_b^0(r)V_\theta^0(r) \\
&= -\frac{4\pi e}{c}\int d^3p\ v_\theta\ f_b^0(H,P_z,P_\theta)\ , \\
\frac{1}{r}\,\frac{\partial}{\partial r}\,r\,\frac{\partial}{\partial r}\,A_z^s(r) &= -\frac{4\pi e}{c}\,n_b^0(r)V_z^0(r) \\
&= -\frac{4\pi e}{c}\int d^3p\ v_z\ f_b^0(H,P_z,P_\theta)\ ,
\end{aligned} \tag{14}$$

where the local ion layer density $n_b^0(r)$ is defined by

$$n_b^0(r)=\int d^3p\ f_b^0(H,P_z,P_\theta)\ . \tag{15}$$

Here, $v_\theta=p_\theta/m_i$, $v_z=p_z/m_i$, and $V_\theta^0(r)$ and $V_z^0(r)$ are the mean azimuthal and axial velocities of an ion layer fluid element.

Substituting Eq. (10) into Eq. (15) and representing $\int d^3p=2\pi\int_{-\infty}^{\infty} dp_\theta\int_0^{\infty} dp_\perp p_\perp$, where $p_\perp^2=p_r^2+(p_z-m_iV_z)^2$, we find that the ion layer density profile is given by

$$n_b^0(r) = \begin{cases} 0, & r<R_1\ , \\ n_b\dfrac{R_0}{r}\ , & R_1<r<R_2\ , \\ 0, & R_2<r<R_c\ , \end{cases} \tag{16}$$

where R_1 and R_2 are the extremes of the interval on which the inequality

$$\psi(r)\geq 0 \tag{17}$$

is satisfied. [That is, R_1 and R_2 are determined from $\psi(R_1)=\psi(R_2)=0$.] In Eq. (17), the envelope function $\psi(r)$ is defined by

$$\psi(r) = \frac{m_i}{2}V_0^2 - \frac{1}{2m_i}\left(\frac{P_0}{r}-\frac{m_i}{2}\omega_{ci}r-\frac{e}{c}A_\theta^s(r)\right)^2+\frac{e}{c}V_zA_z^s(r)\ . \tag{18}$$

It is evident from Eqs. (10) and (18) that

$$H - V_zP_z - \frac{m_i}{2}(V_0^2-V_z^2)$$

$$= \frac{1}{2m_i}[p_r^2+(p_z-m_iV_z)^2]-\psi(r)$$

for $P_\theta=P_0$. That is, $\psi(r)$ is the (r-z) kinetic energy of a layer ion in a frame of reference moving with axial velocity V_z.

Thus far, R_0 has been introduced in the analysis as an unspecified constant parameter in Eq. (10). Without loss of generality, we now choose

R_0 to correspond to that radius where $\psi(r)$ passes through a maximum in the interval $R_1<r<R_2$, i.e.,

$$\left(\frac{\partial}{\partial r}\,\psi(r)\right)_{r=R_0} = 0 \ . \tag{19}$$

Substituting Eq. (18) into Eq. (19), and making use of $\underset{\sim}{B}{}^s_0(\underset{\sim}{r})=B^s_{0\theta}\hat{\underset{\sim}{e}}_\theta+B^s_{0z}\hat{\underset{\sim}{e}}_z=-(\partial/\partial r)A^s_z(r)\hat{\underset{\sim}{e}}_\theta+(1/r)(\partial/\partial r)[rA^s_\theta(r)]\hat{\underset{\sim}{e}}_z$, we obtain

$$\omega_\theta^2+\{\omega_{ci}+[eB^s_{0z}(R_0)/m_ic]\}\omega_\theta-V_zeB^s_{0\theta}(R_0)/m_icR_0=0 \ , \tag{20}$$

where $\omega_\theta=V^0_\theta(R_0)/R_0$ is the angular velocity of an ion layer fluid element at $r=R_0$. Solving Eq. (20) for ω_θ gives $\omega_\theta=\omega^{\pm}_\theta$, where

$$\omega^+_\theta\simeq-\omega_{ci} \ , \tag{21}$$

corresponding to a fast rotational equilibrium with

$$P_0 = -\frac{1}{2}\,m_iR_0^2\omega_{ci}<0 \ . \tag{22}$$

Similarly,

$$\omega^-_\theta\simeq V_zB^s_{0\theta}(R_0)/R_0B_0, \tag{23}$$

corresponding to a slow rotational equilibrium with

$$P_0 = \frac{1}{2}\,m_iR_0^2\omega_{ci}>0 \ . \tag{24}$$

In obtaining Eqs. (21) and (23), use has been made of Eq. (2), which implies weak self fields with $|B^s_\theta|$, $|B^s_z|<<B_0$. Note that there are two classes of equilibria [Eqs. (21)-(24)], namely, a fast rotational equilibrium with $P_0<0$, and a slow rotational equilibrium with $P_0>0$.

A closed analytic determination of R_1 and R_2 from the zeros of Eq. (18) is not generally tractable except for a thin layer [Eq. (1)]. We now spec-

ialize to the case of a thin P-layer with $(R_2-R_1)/R_0<<1$ and Taylor expand Eq. (18) about $r=R_0$, i.e.,

$$\psi(r) = \frac{1}{2} m_i[V_0^2-(P_0/m_iR_0-\omega_{ci}R_0/2)^2] - \frac{1}{2} m_i\omega_r^2(r-R_0)^2+... \tag{25}$$

where

$$\omega_r^2 = - \frac{1}{m_i}\left(\frac{\partial^2\psi}{\partial r^2}\right)_{r=R_0} =\omega_{ci}^2+\omega_b^2\beta^2 \tag{26}$$

is the radial betatron frequency-squared of a layer ion.[13-15] In Eq. (26) $\omega_b^2=4\pi e^2n_b/m_ic$ is the ion plasma frequency-squared, and β^2 is defined by $\beta^2=V_\theta^{02}(R_0)/c^2+V_z^2/c^2=(P_0/m_iR_0c-\omega_{ci}R_0/2c)^2+V_z^2/c^2$. It is important to recognize that the term $\omega_b^2\beta^2$ in Eq. (26) is directly related to the self-field gradients at $r=R_0$. In particular, making use of Eq. (14), it is straightforward to show that $\omega_b^2\beta^2$ can be expressed as

$$\omega_b^2\beta^2 = \omega_{ci}^2 \frac{c^2}{\omega_b^2B_0^2}\left[\left(\frac{\partial B_{0z}^s}{\partial r}\right)^2 + \left(\frac{1}{r}\frac{\partial}{\partial r} rB_{0\theta}^s\right)^2\right]_{r=R_0} .$$

Defining the half thickness of the P-layer by

$$a=[V_0^2-(P_0/m_iR_0-\omega_{ci}R_0/2)^2]^{1/2}/\omega_r , \tag{27}$$

and substituting Eq. (25) into Eq. (17), we readily find $R_1=R_0-a$ and $R_2=R_0+a$, where a is defined in Eq. (27). Finally, we evaluate the angular velocity $\bar{\omega_\theta}$ [Eq. (23)] for a slow rotational equilibrium. Making use of Eq. (14) to eliminate $B_{0\theta}^s(R_0)$, we obtain from Eq. (23)

$$\bar{\omega_\theta}=\nu\omega_{ci}(V_z/R_0\omega_{ci})^2, \tag{28}$$

where $\nu=N_be^2/m_ic^2$ is Budker's parameter defined in Eq. (2), and $N_b=4\pi n_bR_0a$ is the number of layer ions per unit axial length.

For a thin layer, the ion density profile in Eq. (16) can be approximated by

$$n_b^0(r)=\begin{cases} n_b, & |r-R_0|<a \ , \\ \\ 0 \ , & |r-R_0|>a \ . \end{cases} \tag{29}$$

Assuming a space-charge neutralized layer, the layer electron density profile $n_{e'}^0(r)$ is identical to Eq. (29). Moreover, the background plasma has a uniform density profile with

$$n_j^0(r)=n_p, \quad 0<r<R_c, \tag{30}$$

where n_p is constant. We now investigate electrostatic stability properties for perturbations about the plasma-layer equilibrium characterized by Eqs. (9), (10), (25), (29), and (30).

III. ELECTROSTATIC STABILITY PROPERTIES

A. Eigenvalue Equation

In this section, we linearize Eqs. (4)-(7) assuming electrostatic perturbation about the equilibrium described by Eqs. (9), (10), (25), (29), and (30). The present analysis assumes flute perturbations with $\partial/\partial z=0$, so that all perturbations have spatial dependence only on the perpendicular variable $\underset{\sim}{x}_\perp=(r,\theta)$. In the electrostatic approximation, the perturbed electric field is $\delta\underset{\sim}{E}(\underset{\sim}{x},t)=-\nabla_\perp\delta\phi(\underset{\sim}{x},t)$, and Eqs. (4)-(7) can be linearized to give

$$\frac{\partial}{\partial t}\,\delta n_j + \frac{1}{r}\frac{\partial}{\partial r}\,(rn_j^0\delta V_{jr}) + \frac{n_j^0}{r}\frac{\partial}{\partial\theta}\,\delta V_{j\theta}=0\ ,$$

$$\frac{\partial}{\partial t}\,\delta V_{jr} - \varepsilon_j\omega_{cj}\delta V_{j\theta} = -\frac{e_j}{m_j}\frac{\partial}{\partial r}\,\delta\phi\ , \tag{31}$$

$$\frac{\partial}{\partial t}\,\delta V_{j\theta} + \varepsilon_j\omega_{cj}\delta V_{jr} = -\frac{e_j}{m_j}\frac{1}{r}\frac{\partial}{\partial\theta}\,\delta\phi\ ,$$

for the layer electrons and plasma electrons and ions ($j=e',e,i$), and

$$\left\{\frac{\partial}{\partial t} + \underset{\sim}{v}\cdot\frac{\partial}{\partial\underset{\sim}{x}_\perp} + e\left(\underset{\sim}{E}^0(\underset{\sim}{x}) + \frac{\underset{\sim}{v}\times\underset{\sim}{B}_0(\underset{\sim}{x})}{c}\right)\cdot\frac{\partial}{\partial\underset{\sim}{p}}\right\}\delta f_b(\underset{\sim}{x}_\perp,\underset{\sim}{p},t)$$

$$=e[\nabla_\perp\delta\phi(\underset{\sim}{x}_\perp,t)]\cdot\frac{\partial}{\partial\underset{\sim}{p}}\,f_b^0(\underset{\sim}{x}_\perp,\underset{\sim}{p}) \tag{32}$$

for the layer ions ($j=b$). In obtaining Eq. (31), we have approximated $\underset{\sim}{B}_0(\underset{\sim}{x})=B_0\hat{\underset{\sim}{e}}_z$ consistent with Eq. (2). The linearized Poisson equation is

$$\left(\frac{1}{r}\frac{\partial}{\partial r}\,r\,\frac{\partial}{\partial r} + \frac{1}{r^2}\frac{\partial^2}{\partial\theta^2}\right)\delta\phi = -4\pi\left(e\int d^3p\,\delta f_b + \sum_{j=e',e,i} e_j\delta n_j\right)\ , \tag{33}$$

where use has been made of Eq. (9). In Eqs. (31)-(33), $\delta\underset{\sim}{V}_j(\underset{\sim}{x}_\perp,t)$ and $\delta n_j(\underset{\sim}{x}_\perp,t)$ are the perturbed fluid velocity and density, $\delta f_b(\underset{\sim}{x}_\perp,\underset{\sim}{p},t)$ is the perturbed ion layer distribution function, and $\underset{\sim}{E}^0(\underset{\sim}{x}) =-(\partial\phi^0/\partial r)\hat{\underset{\sim}{e}}_r=0$ is the equilibrium radial electric field.

To simplify the right-hand side of Eq. (32), use is made of $\partial P_\theta/\partial \underset{\sim}{p} = r\hat{\underset{\sim}{e}}_\theta$ and $\partial U/\partial \underset{\sim}{p} = \underset{\sim}{v} - V_z \hat{\underset{\sim}{e}}_z$, where $U = H - V_z P_z$. Here $\hat{\underset{\sim}{e}}_\theta$ and $\hat{\underset{\sim}{e}}_z$ are unit vectors in the θ and z directions, respectively. We express perturbed quantities as

$$\delta\psi(\underset{\sim}{x}_\perp, t) = \hat{\psi}_\ell(r)\exp\{i(\ell\theta - \omega t)\}, \quad \mathrm{Im}\,\omega > 0, \tag{34}$$

in Eq. (32), and integrate from $t' = -\infty$ to $t' = t$, using the method of characteristics. In Eq. (34), ω is the complex eigenfrequency, and ℓ is the azimuthal harmonic number. Neglecting initial perturbations, and noting that $\partial f_b^0/\partial U$ and $\partial f_b^0/\partial P_\theta$ are constant (independent of t') along particle trajectories in the equilibrium field configuration, the perturbed ion distribution function can be expressed as

$$\hat{f}_{b\ell}(r, \underset{\sim}{p}) = e\frac{\partial f_b^0}{\partial U}\hat{\phi}_\ell(r) + ie\left(\omega\ \frac{\partial f_b^0}{\partial U} + \ell\ \frac{\partial f_b^0}{\partial P_\theta}\right) I\ , \tag{35}$$

where the orbit integral I is defined by

$$I = \int_{-\infty}^{0} d\tau\ \hat{\phi}_\ell(r')\exp[-i\omega\tau + i\ell(\theta' - \theta)]\ . \tag{36}$$

Here $\tau = t' - t$, and the particle trajectories $\underset{\sim}{x}'(t')$ and $\underset{\sim}{v}'(t')$ satisfy $d\underset{\sim}{x}'/dt' = \underset{\sim}{v}'$ and $m_i d\underset{\sim}{v}'/dt' = e\underset{\sim}{v}' \times \underset{\sim}{B}_0(\underset{\sim}{x}')/c$, with "initial" conditions $\underset{\sim}{x}'(t' = t) = \underset{\sim}{x}$ and $\underset{\sim}{v}'(t' = t) = \underset{\sim}{v}$.

The evaluation of the orbit integral in Eq. (36) is generally complicated. However, for present purposes, we consider low-frequency perturbations satisfying

$$|\omega - \ell\omega_\theta|^2 << \omega_r^2\ ,$$

$$\ell a/R_0 << \omega_r/\omega_{ci}\ , \tag{37}$$

where a is the half-thickness of the layer defined in Eq. (27). Within the context of Eq. (37), it is valid to approximate[15]

$$\hat{\phi}_\ell(r')=\hat{\phi}_\ell(R_0) + \frac{\delta P_\theta}{mR_0}\frac{\omega_0}{\omega_r^2}\left(\frac{\partial\hat{\phi}_\ell}{\partial r}\right)_{r=R_0} ,$$

$$\theta' = \theta + \left(\omega_\theta - \frac{\mu\delta P_\theta}{mR_0^2}\right)\tau , \tag{38}$$

in Eq. (36). In Eq. (38), $\delta P_\theta = P_\theta - P_0$, and

$$\omega_0 = 2P_0/mR_0^2 = \bar{+}\omega_{ci} ,$$

$$\mu = \omega_c^2/\omega_r^2 - 1 = -\omega_b^2\beta^2/\omega_r^2 , \tag{39}$$

where ω_r is the radial betatron frequency defined in Eq. (26), $(\bar{+})$ refers to fast and slow rotational equilibria, and ω_θ is the angular velocity of an ion layer fluid element at $r=R_0$ [$\omega_\theta = \omega_\theta^+ \simeq -\omega_{ci}$ for a fast rotational equilibrium and $\omega_\theta = \omega_\theta^- \simeq \nu\omega_{ci}(V_z/R_0\omega_{ci})^2$ for a slow rotational equilibrium, c.f., Eqs. (21) and (28)]. Substituting Eq. (38) into Eq. (36), and approximating $(v_\theta/r)_{P_\theta=P_0} = \omega_\theta - \omega_0(r-R_0)/R_0$, Eq. (35) can be expressed as

$$\hat{f}_{b\ell}(r,p) = e\frac{\partial f_b^0}{\partial U}\left[\hat{\phi}_\ell(r)-\hat{\phi}_\ell(R_0) - \frac{\ell\omega_0(r-R_0)}{(\omega-\ell\omega_\theta)R_0}\hat{\phi}_\ell(R_0)\right]$$

$$- \frac{ef_b^0}{mR_0(\omega-\ell\omega_\theta)}\left[\frac{\mu\ell^2\hat{\phi}_\ell(R_0)}{R_0(\omega-\ell\omega_\theta)} - \frac{\ell\omega_0}{\omega_r^2}\left(\frac{\partial\hat{\phi}_\ell}{\partial r}\right)_{r=R_0}\right] . \tag{40}$$

We further assume that the ion layer density satisfies

$$n_b \lesssim n_p \tag{41}$$

which will assure the validity of Eq. (37) in the subsequent analysis. To simplify notation, we also introduce the dielectric function of the background plasma

$$\varepsilon(\omega) = 1 - \frac{\omega_{pe}^2}{\omega^2-\omega_{ce}^2} - \frac{\omega_p^2}{\omega^2-\omega_{ci}^2} ,$$
$$\simeq 1 + \frac{\omega_p^2}{\omega_{ce}\omega_{ci}} - \frac{\omega_p^2}{\omega^2-\omega_{ci}^2} , \tag{42}$$

where use has been made of Eq. (37), and $\omega_p^2=4\pi e^2 n_p/m_i$ is the background ion plasma frequency-squared. Substituting Eqs. (34) and (40) into Eqs. (31)-(33), and making use of Eqs. (37) and (42), it is straightforward to express the eigenvalue equation as

$$\frac{1}{r}\frac{\partial}{\partial r}\left[r\varepsilon(\omega)\frac{\partial}{\partial r}\hat{\phi}(r)\right] - \frac{\ell^2}{r^2}\varepsilon(\omega)\hat{\phi}(r) = \frac{\ell\hat{\phi}(r)}{r}\frac{\omega_b^2}{\omega\omega_{ci}}[\delta(r-R_2)-\delta(r-R_1)]$$
$$+ \frac{R_0}{a}\frac{\omega_b^2}{\omega_r^2}\left\{[\hat{\phi}(r)-\hat{\phi}(R_0)] - \frac{\ell\omega_0}{(\omega-\ell\omega_\theta)}\frac{r-R_0}{R_0}\hat{\phi}(R_0)\right\}\left\{\frac{\delta(r-R_1)}{r}\right.$$
$$\left. + \frac{\delta(r-R_2)}{r}\right\} + \omega_b^2\frac{R_0}{r}\Theta[(R_2-r)(r-R_1)]\left[\frac{\mu\ell^2\hat{\phi}(R_0)}{R_0^2(\omega-\ell\omega_\theta)^2}\right.$$
$$\left. - \frac{\ell\omega_0}{R_0\omega_r^2}\left(\frac{\partial\hat{\phi}}{\partial r}\right)_{R_0}\frac{1}{(\omega-\ell\omega_\theta)}\right] , \tag{43}$$

where $\omega_b^2=4\pi e^2 n_b/m_i$, $\hat{\phi}(r)\equiv\hat{\phi}_\ell(r)$, and $\Theta(x)$ is the Heaviside step function defined by

$$\Theta(x)=\begin{cases} 1 , & x\geq 0 . \\ 0 , & x<0 . \end{cases} \tag{44}$$

In obtaining Eq. (43), we have neglected the additional electron layer contribution, $-\omega_{pe}^2,(r)/[\omega^2-\omega_{ce}^2,(r)]$, to the dielectric function $\varepsilon(\omega)$ on the left-hand side of Eq. (43). For the low frequencies considered here, the corresponding term is of order $(n_b/n_p)(m_e/m_i)$ smaller than the plasma ion contribution to $\varepsilon(\omega)$. It should be noted that the terms in Eq. (43) proportional to $\delta(r-R_1)$ and $\delta(r-R_2)$ correspond to surface-charge perturbations on the inner and outer boundaries of the P-layer. These terms have a decisive influence on stability behavior when $\omega_b^2/\omega_{ci}^2>>1$. We further note that the final term

on the right-hand side of Eq. (43) is proportional to $\Theta[(R_2-r)(r-R_1)]$ and corresponds to a body-charge perturbation. The general form of Eq. (43) is similar to the eigenvalue equation obtained by Davidson et al.[15] for a nonrelativistic E-layer, and similar techniques can be used to determine the complex eigenfrequency ω.

B. Dispersion Relation

We now investigate the stability properties predicted by Eq. (43). Since the surface terms in Eq. (43) are nonzero only at the boundaries of the P-layer, the perturbed potential at all other radial points satisfies

$$\left(\frac{1}{r}\frac{\partial}{\partial r}\, r\, \frac{\partial}{\partial r} - \frac{\ell^2}{r^2}\right)\hat{\phi}(r) = \begin{cases} 0\ , & 0<r<R_1\ , \\ \dfrac{\omega_b^2}{\varepsilon R_0 r}\left[\dfrac{\mu\ell^2\hat{\phi}(R_0)}{(\omega-\ell\omega_\theta)^2} - \dfrac{\ell\omega_0 R_0}{\omega_r^2}\dfrac{(\partial\hat{\phi}/\partial r)_{R_0}}{(\omega-\ell\omega_\theta)}\right], & R_1<r<R_2\ , \\ 0\ , & R_2<r<R_c\ , \end{cases} \tag{45}$$

where $R_1=R_0-a$ and $R_2=R_0+a$ are the boundaries of the P-layer. For $\ell\geq 2$, the physically acceptable solution to Eq. (45) is

$$\hat{\phi}(r) = \begin{cases} Ar^{\ell}\ , & 0<r<R_1\ , \\ Br^{\ell}+cr^{-\ell} - \dfrac{\omega_b^2/\varepsilon}{\ell^2-1}\dfrac{r}{R_0}\left[\dfrac{\mu\ell^2\hat{\phi}(R_0)}{(\omega-\ell\omega_\theta)^2} - \dfrac{\ell\omega_0 R_0(\partial\hat{\phi}/\partial r)_{R_0}}{\omega_r^2(\omega-\ell\omega_\theta)}\right], & R_1<r<R_2\ , \\ Dr^{\ell}+Er^{-\ell}\ , & R_2<r<R_c\ , \end{cases}$$

where A, B, C, D, and E are constants. For $\ell=1$, the solution to Eq. (45) can be expressed as

$$\hat{\phi}(r) = \begin{cases} A'r\ , & 0<r<R_1\ , \\ B'r+C'r^{-1} + \dfrac{1}{2}\dfrac{\omega_b^2}{\varepsilon}\dfrac{r}{R_0}\left[\dfrac{\mu\hat{\phi}(R_0)}{(\omega-\omega_\theta)^2} - \dfrac{\omega_0 R_0(\partial\hat{\phi}/\partial r)_{R_0}}{\omega_r^2\,(\omega-\omega_\theta)}\right], & R_1<r<R_2\ , \\ D'r+E'r^{-1}\ , & R_2<r<R_c\ , \end{cases}$$

where A', B', C', D', and E' are constants. Since Eq. (43) is similar in general form to Eq. (88) of Ref. 15, we briefly outline the derivation of the dispersion relation. [The detailed procedure is similar to Ref. 15.]

We introduce the abbreviated notation

$$
\begin{aligned}
S_1(\omega) &= \frac{R_0}{a\varepsilon}\frac{\omega_b^2}{\omega_r^2}\,, \\
S_2(\omega) &= -\frac{\omega_b^2}{\omega_r^2\varepsilon}\frac{\ell\omega_0}{(\omega-\ell\omega_\theta)}\,, \\
S_3(\omega) &= \frac{\ell\omega_b^2}{\varepsilon\omega\omega_{ci}}\,, \\
N_1(\omega) &= \mu\frac{\ell^2}{\ell^2-1}\frac{\omega_b^2/\varepsilon}{(\omega-\ell\omega_\theta)^2}\,, \\
N_2(\omega) &= -\frac{1}{\ell^2-1}\frac{(\omega_b^2/\varepsilon)\ell\omega_0}{\omega_r^2(\omega-\ell\omega_\theta)}\,.
\end{aligned}
\tag{46}
$$

Three constraints relating the constants A, B, C, D, and E (or A', B', C', D', and E') are obtained from the boundary condition $\hat{\phi}(r=R_c)=0$, and by enforcing continuity of $\hat{\phi}(r)$ at $r=R_1$ and $r=R_2$. The remaining two constraints are obtained by integrating Eq. (43) across the layer boundaries at $r=R_1$ and at $r=R_2$. After some tedious algebra, we obtain the dispersion relation

$$
\begin{aligned}
&\left\{4\ell^2 g_f+2\ell(S_1+S_3)+2\ell(S_1-S_3)\left(\frac{R_1}{R_2}\right)^{2\ell}+(2\ell g_f+S_1+S_3)(S_1-S_3)\left[1-\left(\frac{R_1}{R_2}\right)^{2\ell}\right]\right\} \\
&\times(1+N_1+N_2)+(2\ell g_f+S_1+S_3)(\chi_1-\chi_3)\left(\frac{R_1}{R_0}\right)^{\ell}-(2\ell+S_1-S_3)(\chi_2+\chi_4)\left(\frac{R_0}{R_2}\right)^{\ell} \\
&+(S_1-S_3)(\chi_2-\chi_4)\left(\frac{R_1^2}{R_0R_2}\right)^{\ell}-[2\ell(g_f-1)+(S_1+S_3)(\chi_1+\chi_3)]\left(\frac{R_1R_0}{R_2^2}\right)^{\ell}
\end{aligned}
$$

$$+2\ell N_2\left(\frac{R_1}{R_2}\right)^{\ell}\left[\left(\frac{R_1}{R_0}\right)(1-\ell-S_1+S_3)(S_1-S_2)+\left(\frac{R_2}{R_0}\right)(1-\ell+2\ell g_f+S_1+S_3)(S_1+S_2)\right]=0, \tag{47}$$

for $\ell\geq 2$. In Eq. (47), $\chi_j(\omega)$ is defined by

$$\begin{aligned}
\chi_1(\omega) &= \frac{R_1}{R_0}(1-\ell-S_1+S_3)N_1-(S_1+S_2)(1+N_2)\ , \\
\chi_2(\omega) &= \frac{R_2}{R_0}(1-\ell+2\ell g_f+S_1+S_3)N_1+(S_1-S_2)(1+N_2)\ , \\
\chi_3(\omega) &= \left[\frac{R_1}{R_0}(1-\ell-S_1+S_3)+S_1+S_2\right]\ell N_2\ , \\
\chi_4(\omega) &= \left[\frac{R_2}{R_0}(1-\ell+2\ell g_f+S_1+S_3)-S_1+S_2\right]\ell N_2\ ,
\end{aligned} \tag{48}$$

and the geometric factor g_f is defined by

$$g_f=[1-(R_2/R_c)^{2\ell}]^{-1}\ . \tag{49}$$

Equation (47) is the desired dispersion relation for $\ell\geq 2$. Keep in mind that $\ell<<R_0/a$ has been assumed in deriving Eq. (47) [see Eq. (37)]. Substituting $R_1=R_0-a$ and $R_2=R_0+a$, and Taylor expanding the left-hand side of Eq. (47), for $a<<R_0$, we find that the dispersion relation can be approximated by

$$\Gamma_1 x^2+\Gamma_2\frac{\omega_b^2}{\varepsilon\omega_r^2}\frac{a}{R_0}x+\Gamma_3\frac{\omega_b^2}{\varepsilon\omega_{ci}^2}\frac{\ell a}{R_0}=0\ , \tag{50}$$

where

$$x=(\omega-\ell\omega_\theta)/\omega_{ci} \tag{51}$$

is the normalized Doppler-shifted eigenfrequency, Γ_j is defined by

$$\Gamma_1(g_f,\omega)=g_f\left(1+\frac{\omega_b^2}{\varepsilon\omega_r^2}\right)+\frac{\ell}{2}\left(\frac{\omega_b^2}{\varepsilon\omega_r^2}\right)^2\frac{a}{R_0}\,,$$

$$\Gamma_2(g_f,\omega)=\left(2+\frac{\omega_b^2}{\varepsilon\omega_r^2}\right)\left[\ell(g_f-1)+\frac{\omega_b^2}{\varepsilon\omega\omega_{ci}}\right]-\frac{\omega_b^2}{2\varepsilon\omega_r^2}\,, \qquad (52)$$

$$\Gamma_3(\omega)=\mu\left(1+\frac{3}{2}\frac{\omega_b^2}{\varepsilon\omega_r^2}+\frac{\omega_b^4}{\varepsilon^2\omega_r^4}\right)-\frac{\omega_c^2}{\omega_r^2}\left(\frac{\omega_b^2}{\varepsilon\omega_r^2}+\frac{\omega_b^4}{\varepsilon^2\omega_r^4}\right),$$

and $(\bar{+})$ refers to fast and slow rotational equilibria. In obtaining Eq. (50), use has been made of the definitions in Eqs. (39), (46), and (48).

The preceding analysis pertains to $\ell\geq 2$. A similar procedure can be followed to obtain the dispersion relation for $\ell=1$. After some algebraic manipulation, it is straightforward to show in the thin-layer approximation that the dispersion relation in Eq. (50) is also valid for $\ell=1$. In this context, Eq. (50) is the desired dispersion relation, which determines the electrostatic stability properties for $1\leq\ell<<R_0/a$.

IV. STABILITY ANALYSIS

We now investigate the stability properties predicted by Eqs. (50)-(52). The stability analysis for a slow rotational equilibrium proceeds in the following manner. Since the angular velocity of an ion layer fluid element for a slow rotational equilibrium is much less than the ion cyclotron frequency, i.e.,

$$\bar{\omega_\theta}=\nu\omega_{ci}(V_z/R_0\omega_{ci})^2<<\omega_{ci} ,$$

it is readily shown from Eq. (42) that the background plasma dielectric function can be approximated by

$$\varepsilon(\ell\bar{\omega_\theta})\simeq 1+(1+\omega_{ci}/\omega_{ce})(\omega_p^2/\omega_{ci}^2)>0 . \tag{53}$$

Substituting Eq. (53) into Eq. (52), yields the inequalities

$$\Gamma_1(g_f,\ell\bar{\omega_\theta})>0, \quad \Gamma_3(\ell\bar{\omega_\theta})<0 . \tag{54}$$

Within the context of Eqs. (50), (53), and (54), it is straightforward to show that the system is stable for a slow rotational equilibrium.

The stability analysis for a fast rotational P-layer is generally more complicated. We therefore restrict the analysis to

$$\omega_p^2>>\omega_{ci}^2 . \tag{55}$$

Making use of $n_p\gtrsim n_b$ in Eq. (41), it is straightforward to show that

$$|\omega_b^2\Gamma_2^2/\ell\Gamma_1\Gamma_3\varepsilon\omega_{ci}^2|\lesssim 1.$$

In this context, the dispersion relation can be approximated by

$$\Gamma_1 x^2+\Gamma_3\frac{\omega_b^2}{\varepsilon\omega_{ci}^2}\frac{\ell a}{R_0}=0 , \tag{56}$$

where the term proportional to x has been neglected. Moreover, making use of the inequality in Eq. (37) the dielectric function in Eq. (42) can be approximated by

$$\varepsilon(\omega) \simeq -\left(\frac{\omega_p^2}{\omega_{ci}^2}\right) \begin{cases} (x^2-2x)^{-1} , & \ell=1 , \\ [x^2-2\ell x+(\ell^2-1)]^{-1} , & \ell \geq 2 , \end{cases} \tag{57}$$

where $x=(\omega-\ell\omega_\theta^+)/\omega_{ci} \simeq (\omega+\ell\omega_{ci})/\omega_{ci}$.

A general numerical analysis of Eqs. (56) and (57) is summarized later in this section. However, for eigenfrequencies satisfying

$$|\omega+\ell\omega_{ci}| << \omega_{ci} , \tag{58}$$

Eq. (57) can be further simplified to give

$$\varepsilon(\omega) \simeq -\left(\frac{\omega_p}{\omega_{ci}}\right)^2 \begin{cases} -(2x)^{-1} , & \ell=1 , \\ (\ell^2-1)^{-1} , & \ell \geq 2 , \end{cases} \tag{59}$$

and the solution to Eq. (56) is analytically tractable. Defining

$$y=(\ell^2-1)(n_b/n_p)(\omega_{ci}/\omega_r)^2 ,$$

$$q=(\omega_r^2-\omega_{ci}^2)/\omega_{ci}^2=\omega_b^2\beta^2/\omega_{ci}^2 , \tag{60}$$

Eq. (56) can be expressed as

$$(1-y)x^2 + \frac{\ell a}{R_0}\left[1-\left(\frac{R_0}{R_c}\right)^{2\ell}\right] y\left[(q+1)y^2-\left(\frac{3}{2}q+1\right)y+q\right]=0 , \tag{61}$$

for $\ell \geq 2$. Here, q is a measure of the strength of the self-field gradients at $r=R_0$. [See expression for $\omega_b^2\beta^2$ following Eq. (26).] In obtaining Eq. (61), use has been made of Eqs. (1), (26), (39), (49), and (59). Note from Eq. (60) that y is positive for $\ell \geq 2$.

A parallel analysis for $\ell=1$ results in a dispersion relation with stable solutions in the parameter regime of physical interest. We therefore restrict discussion to mode numbers $\ell \geq 2$.

We note from Eq. (61) that $(q+1)y^2-(3q/2+1)y+q \geq q/2$ for $y \geq 1$. Therefore, the necessary and sufficient conditions for instability can be expressed as

$$y<1 \ , \tag{62}$$

and

$$(1+q)y^2-\left(\frac{3}{2}\ q+1\right)y+q>0 \ , \tag{63}$$

for $\ell \geq 2$ and $|\omega+\ell\omega_{ci}| << \omega_{ci}$. It is straightforward to show that Eq. (63) is automatically satisfied for

$$q=\omega_b^2\beta^2/\omega_{ci}^2>2(2^{3/2}-1)/7=0.52. \tag{64}$$

For the case $q>0.52$, the necessary and sufficient condition for instability is given by $y<1$ in Eq. (62). It should be noted from Eqs. (62) and (63) that the stability criteria are independent of the location of the conducting wall. Moreover, the system is stable when the self field is negligibly small, i.e., $q<<1$. Finally, we note that the maximum growth rate occurs at the resonant value

$$(n_b/n_p)=(1+q)/(\ell^2-1) \ , \tag{65}$$

corresponding to $y=1$.

Removing the restriction in Eq. (58), the dispersion relation in Eq. (56) has been solved numerically by substituting Eq. (57) into Eq. (56). Figure 2 shows a plot of the normalized growth rate $\mathrm{Im}\omega/\omega_{ci}=\omega_i/\omega_{ci}$ versus n_b/n_p for $\ell=2$, $a/R_0=0.05$, $R_0/R_c=0.5$, and several values

of q. Several points are noteworthy in Fig. 2. First, the instability growth rate is considerably increased when the strength of the self magnetic field (as measured by q) is increased. For example, the maximum growth rate $(\omega_i)_m=0.114\ \omega_{ci}$ for q=0.5 occurs at $n_b/n_p=0.63$, while the maximum growth rate $(\omega_i)_m=0.25\ \omega_{ci}$ for q=2 occurs at $n_b/n_p=0.65$. We also note that the value of n_b/n_p corresponding to maximum growth increases as the self magnetic field is increased [see also Eq. (65)]. Second, the maximum growth rate can be a substantial fraction of the ion cyclotron frequency ω_{ci}. Third, even for weak self-field effects (q<1), the range of n_b/n_p corresponding to instability is considerably extended beyond the range of n_b/n_p predicted by Eq. (62). For example, for q=0.5, Eq. (62) predicts that instability occurs only for $n_b/n_p\leq 0.5$. On the other hand, from Fig. 2, we note that the system is unstable for values of n_b/n_p up to $n_b/n_p=1.6$. However, the absolute maximum growth rate does occur very near to the resonant value of n_b/n_p (for example, $n_b/n_p=0.5$, for q=0.5) [Eq. (65)]. Fourth, the growth rate curve has more than one maximum for $q\leq 0.52$, which is predicted by Eq. (63). [See the curves corresponding to q=0.25 and q=0.5 in Fig. 2.] We also emphasize that the range of n_b/n_p corresponding to instability is rapidly reduced when the azimuthal harmonic number ℓ is increased.

Of considerable interest for experimental application is the stability behavior for specified values of n_b/n_p, q, and R_0/R_c. Typical results are shown in Fig. 3 where $Im\omega/\omega_{ci}$ is plotted versus mode number ℓ for $n_b/n_p=0.1$, $a/R_0=0.05$, $R_0/R_c=0.5$, and several values of q. From Fig. 3, we note that the number of unstable modes increases as the self-field strength (as measured by q) is increased. For example, for q=2, the mode numbers from $\ell=2$ to $\ell=7$ are unstable. On the other hand, for q=0.25, only the $\ell=4$ mode is unstable. Moreover, the maximum

growth rate is increased by increasing the value of q.

We conclude this section by emphasizing that the growth rate exhibits a sensitive dependence on the location of the conducting wall. This is illustrated in Fig. 4 where the normalized growth rate $Im\omega/\omega_{ci}$, and the normalized Doppler-shifted real frequency $Re(\omega+\ell\omega_{ci})/\omega_{ci}$ are plotted versus R_0/R_c for $\ell=3$, $n_b/n_p=0.2$, $a/R_0=0.05$, and several values of q. Evidently, the growth rates as well as the Doppler shifted real frequencies are substantially reduced whenever the conducting wall is located sufficiently close to the P-layer.

V. CONCLUSIONS

In this paper, we have investigated the electrostatic stability properties of a rotating P-layer immersed in a uniform background plasma. The equilibrium and stability analysis (Secs. II-IV) was carried out within the framework of a hybrid (Vlasov-fluid) model in which the layer ions are described by the Vlasov equation, and the layer electrons and background plasma electrons and ions are described as a macroscopic, cold fluid. Moreover, electrostatic stability properties were calculated for the choice of equilibrium ion distribution function in Eq. (10). Although a slow rotational equilibrium ($P_0>0$) is stable [see discussion following Eq. (54)], it is found [Sec. IV] that a high-density fast rotational equilibrium ($P_0<0$) is unstable for a broad range of physical parameters. One of the most important conclusions of this study is that the background plasma has a large influence on stability behavior. In particular, the instability growth rate is significantly reduced for sufficiently low background plasma density. Finally, we conclude that the growth rate increases with increasing self-magnetic field (as measured by q). Moreover, the characteristic growth rate for $\ell \geq 2$ is a substantial fraction of the ion cyclotron frequency. The fundamental mode ($\ell=1$), however, is found to be stable.

ACKNOWLEDGMENTS

This research was supported by the National Science Foundation. The research by one of the authors (H.S.U.) was supported in part by the Office of Naval Research under the auspices of the University of Maryland-Naval Research Laboratory Joint Program in Plasma Physics.

REFERENCES

1. S. Humphries, T. J. Lee, and R. N. Sudan, J. Appl. Phys. 46, 187 (1975).
2. S. Humphries, R. N. Sudan, and L. Willey, J. Appl. Phys. 47, 2382 (1976).
3. C. A. Kapetanakos, J. Golden, and F. C. Young, Nucl. Fusion 16, 151 (1976).
4. C. A. Kapetanakos, J. Golden, and W. M. Black, Phys. Rev. Lett. 37, 1236 (1976).
5. S. J. Stephanakis, D. Mosher, G. Cooperstein, J. R. Roller, J. Golden, and S. A. Goldstein, Phys. Rev. Lett. 37, 1543 (1976).
6. J. Golden, C. A. Kapetanakos, S. J. Marsh, and S. J. Stephanakis, Phys. Rev. Lett. 38, 130 (1977).
7. R. N. Sudan and E. Ott, Phys. Rev. Lett. 33, 355 (1974).
8. C. A. Kapetanakos, R. K. Parker, and K. R. Chu, Appl. Phys. Lett. 26, 284 (1975).
9. C. A. Kapetanakos, J. Golden, and K. R. Chu, Plasma Phys. 19, 387 (1977).
10. R. V. Lovelace, Phys. Rev. Lett. 35, 162 (1975).
11. R. N. Sudan and M. N. Rosenbluth, Phys. Rev. Lett. 36, 972 (1976).
12. H. L. Berk, L. D. Pearlstein, and G. M. Walters, Phys. Fluids 13, 2141 (1970).
13. H. Uhm and R. C. Davidson, Phys. Fluids 20, 771 (1977).
14. H. S. Uhm and R. C. Davidson, Phys. Fluids 21, 265 (1978).
15. R. C. Davidson, H. Uhm, and S. M. Mahajan, Phys. Fluids 19, 1608 (1976).
16. R. C. Davidson, Theory of Nonneutral Plasmas (W. A. Benjamin, Reading, Mass., 1974), Ch. 2.

FIGURE CAPTIONS

Fig. 1 Equilibrium configuration and coordinate system.

Fig. 2 Plots of normalized growth rate $\mathrm{Im}\omega/\omega_{ci}$ versus n_b/n_p obtained from Eq. (56) for $\ell=2$, $a/R_0=0.05$, $R_0/R_c=0.5$, and several values of q.

Fig. 3 Plots of normalized growth rate $\mathrm{Im}\omega/\omega_{ci}$ versus ℓ obtained from Eq. (56) for $n_b/n_p=0.1$, $a/R_0=0.05$, $R_0/R_c=0.5$, and several values of q.

Fig. 4 Plots of (a) normalized growth rate $\mathrm{Im}\omega/\omega_{ci}$, and (b) normalized real frequency $\mathrm{Re}(\omega+\ell\omega_{ci})/\omega_{ci}$ versus R_0/R_c obtained from Eq. (56) for $\ell=3$, $n_b/n_p=0.2$, $a/R_0=0.05$, and several values of q.

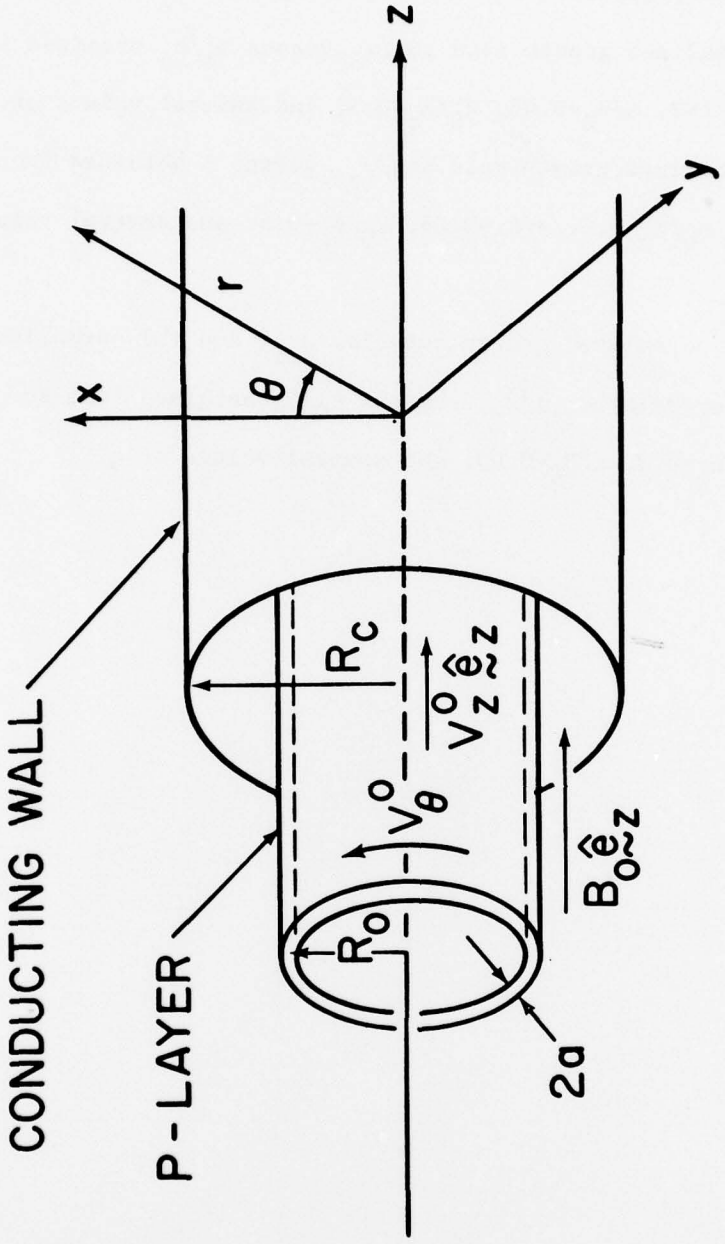
z
y
x
r
θ
CONDUCTING WALL
P-LAYER
R_c
R_o
V_θ^o
$V_z^o \hat{e}_z$
$B_o \hat{e}_z$
2a

Fig. 1

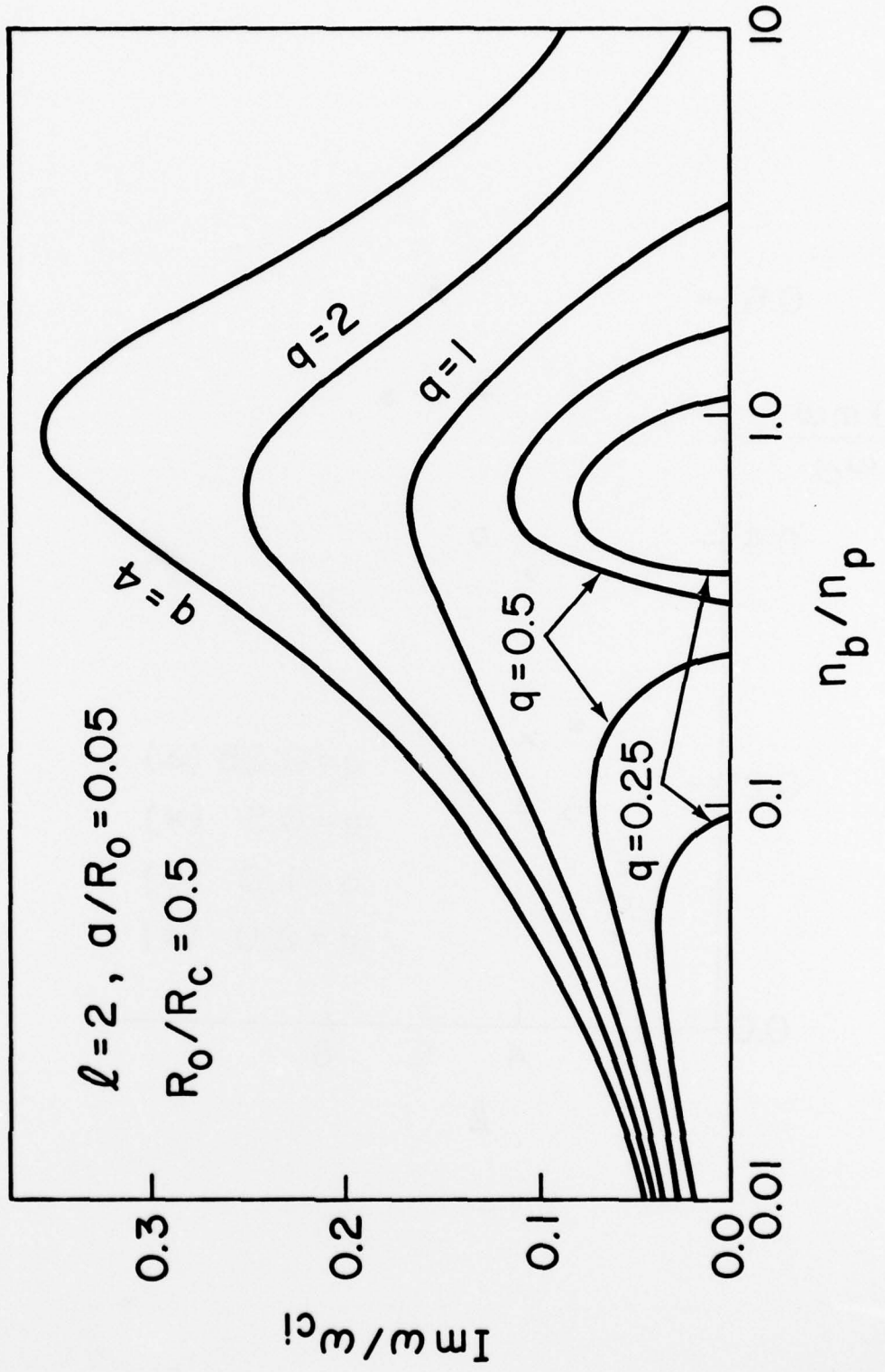
ℓ=2, a/R0=0.05
R0/Rc=0.5
q=4
q=2
q=1
q=0.5
q=0.25
Imω/ωci
nb/np
0.0
0.1
0.2
0.3
0.01
0.1
1.0
10

Fig. 2

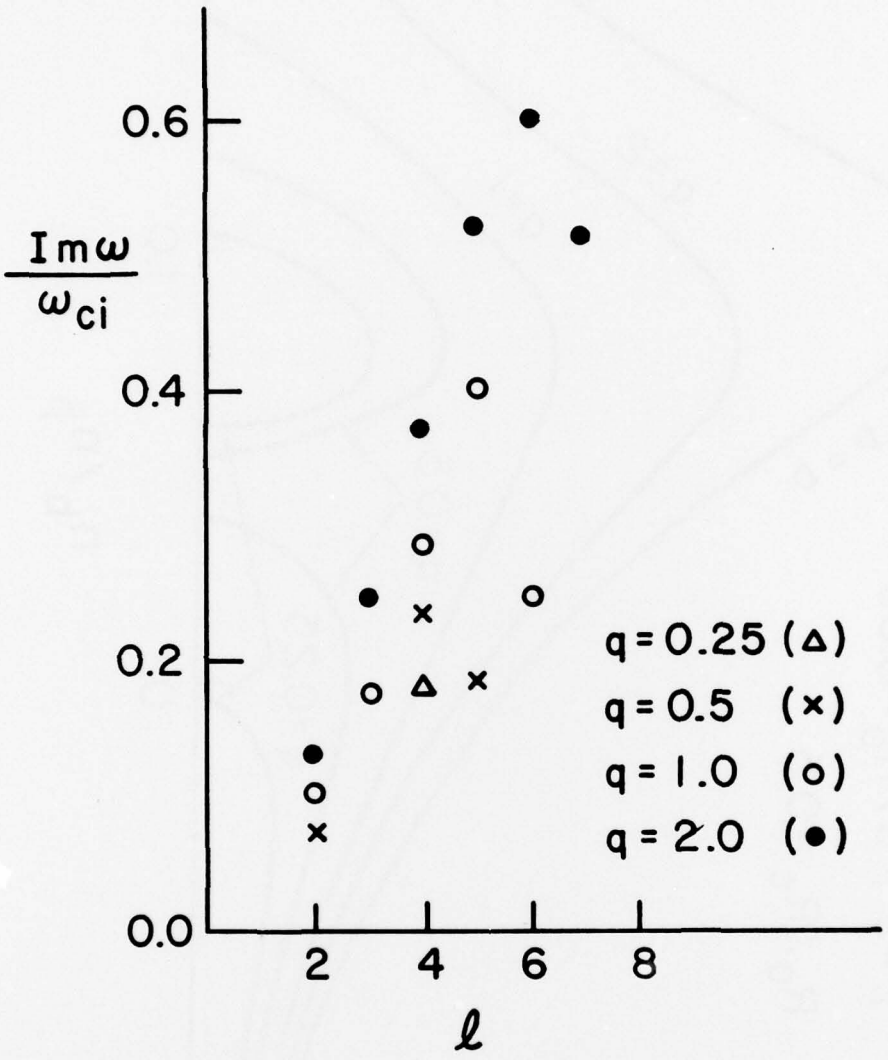

Fig. 3

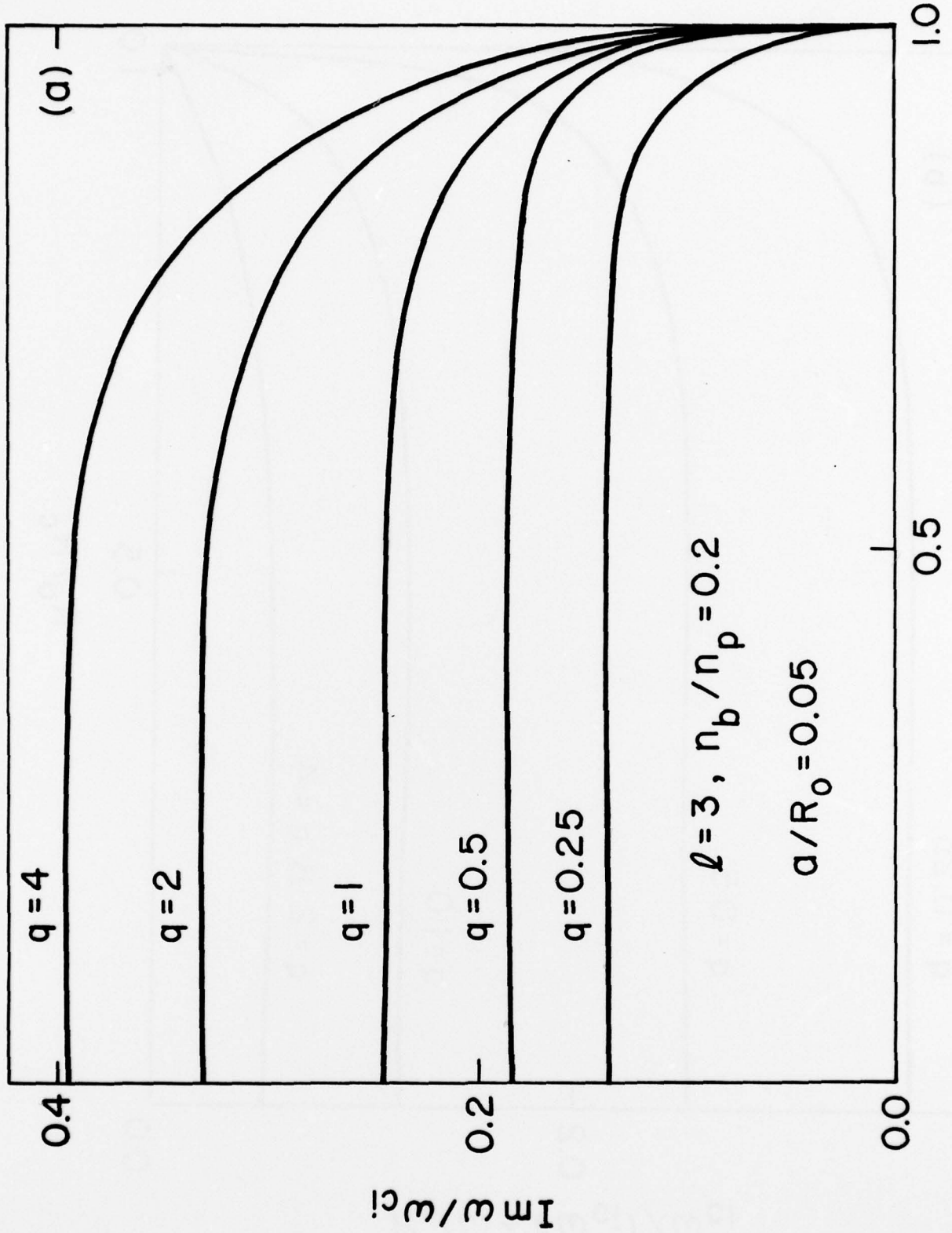
(a)
q=4
q=2
q=1
q=0.5
q=0.25
ℓ=3, n_b/n_p=0.2
a/R_o=0.05
0.4
0.2
0.0
1.0
0.5
R_o/R_c
$Im\,\omega/\omega_{ci}$

Fig. 4a

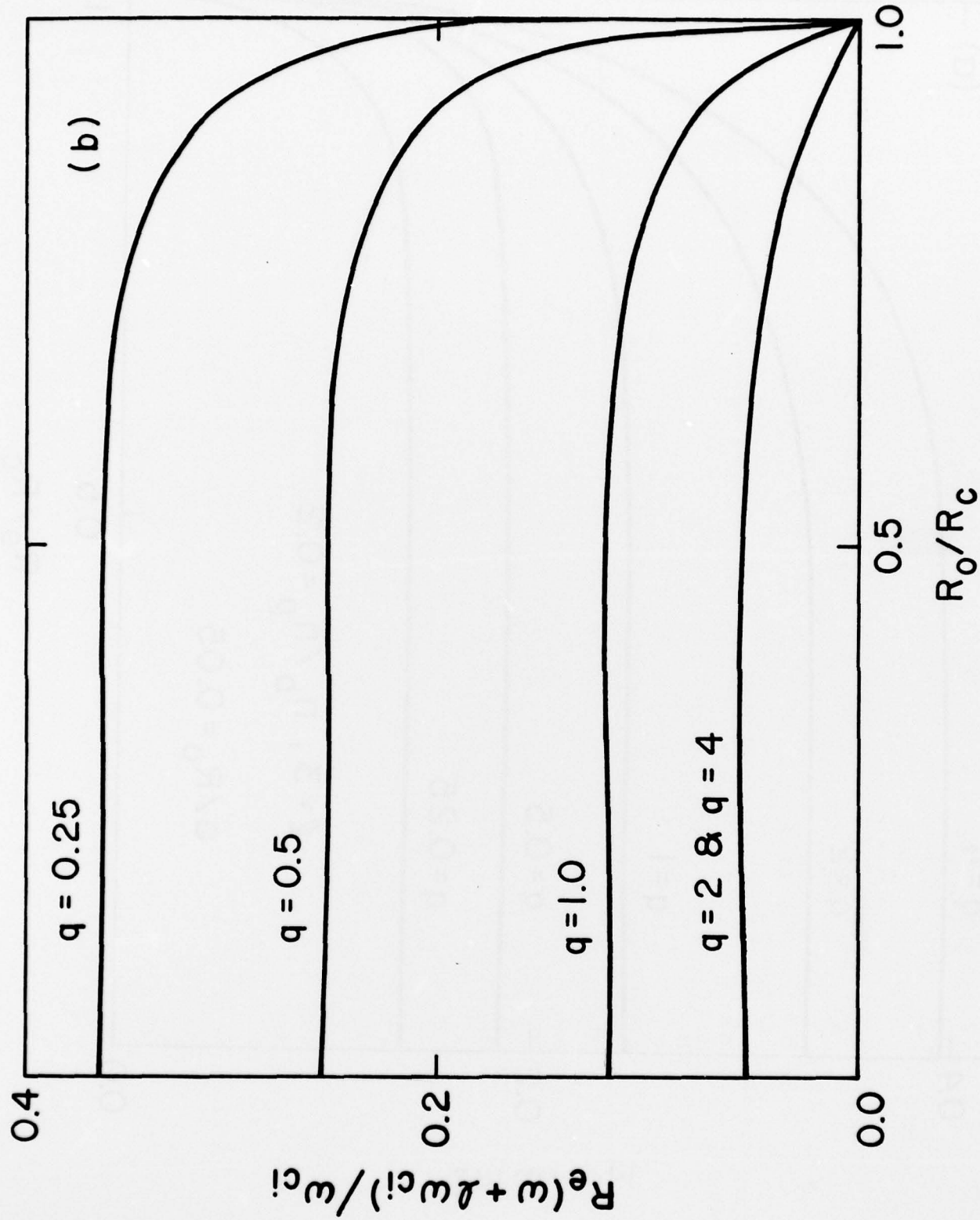
(b)
q = 0.25
q = 0.5
q=1.0
q=2 & q = 4
0.4
0.2
0.0
0.5
1.0
R_o/R_c
$R_e(\omega + \lambda\omega_{ci})/\omega_{ci}$

Fig. 4b